

Analyst

Accepted Manuscript

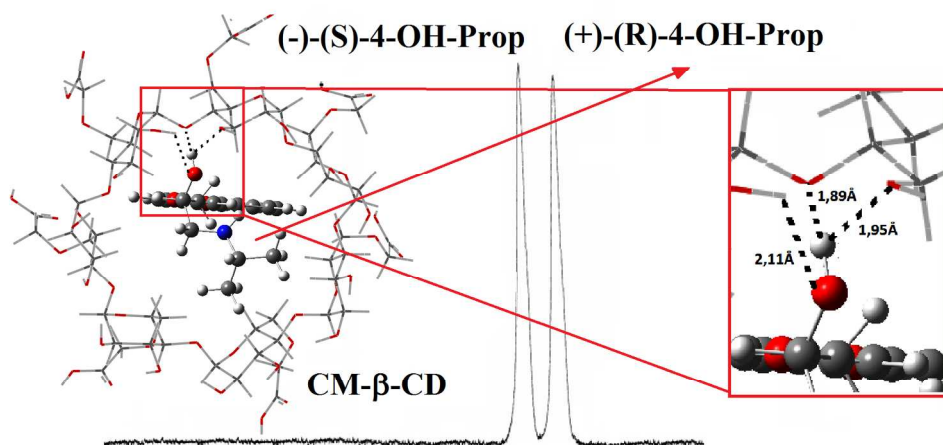


This is an *Accepted Manuscript*, which has been through the Royal Society of Chemistry peer review process and has been accepted for publication.

Accepted Manuscripts are published online shortly after acceptance, before technical editing, formatting and proof reading. Using this free service, authors can make their results available to the community, in citable form, before we publish the edited article. We will replace this *Accepted Manuscript* with the edited and formatted *Advance Article* as soon as it is available.

You can find more information about *Accepted Manuscripts* in the [Information for Authors](#).

Please note that technical editing may introduce minor changes to the text and/or graphics, which may alter content. The journal's standard [Terms & Conditions](#) and the [Ethical guidelines](#) still apply. In no event shall the Royal Society of Chemistry be held responsible for any errors or omissions in this *Accepted Manuscript* or any consequences arising from the use of any information it contains.



Graphical Abstract
527x270mm (96 x 96 DPI)

1
2
3 **Molecular modeling study of the recognition mechanism and enantioseparation of**
4 **4-hydroxypropranolol by capillary electrophoresis using carboxymethyl- β -**
5 **cyclodextrin as chiral selector**
6
7

8
9 Clebio Soares Nascimento Júnior^{1*}, Juliana Fedoce Lopes², Luciana Guimarães¹,
10 Keyller Bastos Borges^{1*}
11

12
13
14 ¹ Departamento de Ciências Naturais, Universidade Federal de São João del-Rei,
15 Campus Dom Bosco, Praça Dom Helvécio 74, Fábricas, 36301-160, São João del-Rei,
16 Minas Gerais, Brazil
17
18

19
20 ² Departamento de Física e Química, Instituto de Ciências Exatas, Universidade Federal
21 de Itajubá, Campus Professor José Rodrigues Seabra, Av. BPS 1303, Pinheirinho,
22 37500-903, Itajubá, Minas Gerais, Brazil
23
24
25
26
27

28
29 ***Correspondence:**
30

31
32 Dr. Keyller Bastos Borges, Departamento de Ciências Naturais, Universidade Federal
33 de São João del-Rei, Campus Dom Bosco, Praça Dom Helvécio 74, Fábricas, 36301-
34 160, São João del-Rei, Minas Gerais, Brazil
35

36
37 e-mail: keyller@ufsj.edu.br
38

39
40 Dr. Clebio Soares Nascimento Júnior, Departamento de Ciências Naturais, Universidade
41 Federal de São João del-Rei, Campus Dom Bosco, Praça Dom Helvécio 74, Fábricas,
42 36301-160, São João del-Rei, Minas Gerais, Brazil
43
44

45
46 e-mail: clebio@ufsj.edu.br
47

48
49
50
51 Tel.: +55 32 3379 – 2483
52

53
54 Fax: +55 32 3379 – 2483
55
56
57
58
59
60

ABSTRACT

The purpose of this paper was to study in molecular level the enantioseparation mechanism of 4-hydroxypropranolol (4-OH-Prop) with carboxymethyl- β -cyclodextrin (CM- β -CD) using a sequential methodology which included Molecular Dynamics simulations (MD) Parametric Model 3 semiempirical (PM3) and Density Functional Theory (DFT) calculations. As results, a systematic structural analysis indicated that hydrogen bonds formed between host and guests play a major role on the complex stabilization. The inclusion complex (+)-(R)-4-OH-Prop/CM- β -CD showed three strong intermolecular hydrogen bonds. Moreover, the guest inclusion process made from wider CD rim presented lower energies (interaction and Gibbs free energy) in comparison to the inclusion made by narrower CD rim both in gas and aqueous phases. This difference in energies of drug/CM- β -CD inclusion complexes is probably a measure of chiral discrimination, which results in the separation of the enantiomers and the distinct separation factors as observed in previous experimental findings. Comparing the experimental results of the separation of 4-OH-Prop enantiomers by Capillary Electrophoresis (CE), the proposed theoretical model demonstrated good capability to predict chiral separation of 4-OH-Prop enantiomers as well as the qualitative estimative of chiral recognition mechanism.

Keywords: Molecular modeling, Theoretical Calculations, Cyclodextrins, Enantioseparation, 4-hydroxypropranolol, Capillary electrophoresis

1. Introduction

Analytical methods such as Thin Layer Chromatography (TLC), High Performance Liquid Chromatography (HPLC) and Capillary Electrophoresis (CE) have attracted great interest in chiral separations of β -adrenergic antagonists class of compounds [1-6]. Among these analytical methods, CE has excelled due to their advantages for chiral separations, such as: (i) separation efficiency; (ii) low solvent; (iii) selector consumption and (iv) ability to readily change the types and concentration of chiral selectors.

The enantioseparation process can be performed using chiral selectors. This process consists in an enantioselective complexation between the enantiomers of the analyte and the chiral selector, giving rise to differences in the electrophoretic mobility of the enantiomers. In this sense, various chiral selectors such as polysaccharides, proteins, cyclodextrins (CDs), chiral crown ethers, chiral surfactants are currently available. Among them, CDs are the most widely used due to their excellent chiral recognition abilities [7,8]. When CDs are used as chiral selectors, the chiral recognition mechanism is usually based on inclusion complexation where the analyte fits into the CD cavity. The studies dealing with the enantiomer migration order (EMO) in CE are important from the mechanistic point of view. The concept here is that understanding the nature of the forces responsible for the each enantiomer affinity pattern means an elucidation of chiral recognition mechanisms of chiral selectors.

In last years, some works [9,10] have pointed out the chiral recognition mechanisms of β -adrenergic antagonists with CDs using Nuclear Magnetic Resonance (NMR), however detailed mechanisms concerning to the enantioseparation remain still not understood. The fundamental issue is the difficult to explain the influence of hydrogen bonding in the chiral recognition process due to the limitations of the

1
2
3 experimental methods to describe the molecular level scenario. In this sense, molecular
4
5 modeling can be a useful tool in order to rationalize experimental findings. One of the
6
7 strengths of theoretical investigation is the ability to generate data, in which an
8
9 experimentalist may gain insight and thus rationalize the behavior of determined
10
11 physical and chemical phenomena. In recent years, several molecular modeling studies
12
13 have emerged in literature in order to investigate the interaction of inclusion complexes
14
15 between CDs and enantiomers and then to elucidate chiral recognition processes [11-
16
17 16]. Furthermore, there are some theoretical works regarding the EMO using CDs as
18
19 chiral selectors [17-19].
20
21
22

23 The elucidation of EMO in CE is a constant problem for the analysts. EMO is
24
25 not a popular topic in chiral CE [20,21]. Currently, there is not an instrument of CE with
26
27 polarimetric or circular dichroism detector available which can provide *on-line*
28
29 information regarding EMO. The small diameter of capillary requires a highly sensitive
30
31 detector and the presence of chiral selector in high concentrations (100 fold compared to
32
33 analytes) create serious problems for on-line determination of the EMO in CE [21]. So,
34
35 to study the EMO in CE require at least one of the enantiomers optically pure or
36
37 enriched form. Not all analytes are commercially available in enantiomerically pure
38
39 form, and when available, they may be quite expensive [21]. Using the molecular
40
41 modeling technique, analysts may be able to understand in advance whether a chiral
42
43 discrimination could be achieved with a given chiral selector, and then select an
44
45 appropriate chiral selector and predict the result of enantioseparation.
46
47
48

49 Among different metabolites of propranolol (Prop), 4-hydroxypropranolol (4-
50
51 OH-Prop) was reported to be one of major metabolites in humans and animals. 4-OH-
52
53 Prop was first identified in urine of humans and several animal species [22]. Later, it
54
55 was identified as an equipotent to Prop for its β -adrenoreceptor blocking activity
56
57
58
59
60

1
2
3 [23,24]. 4-OH-Prop reaches similar peak plasma concentration in man after an oral
4
5 administration of Prop but has a significant shorter half-life [25,26]. As that of Prop it
6
7 gets extensively metabolized in human liver and excreted mainly as a glucuronic acid
8
9 and sulfate conjugate [25,27–29].
10

11
12 In this context, to understand the possible chiral recognition mechanisms of 4-
13
14 OH-Prop enantiomers with carboxymethyl- β -cyclodextrin (CM- β -CD), host-guest
15
16 binding procedures of CM- β -CD and 4-OH-Prop enantiomers (Fig. 1) were studied in
17
18 the present work by Molecular Dynamic Simulations (MD), Parametric Model 3 (PM3)
19
20 semiempirical and Density Functional Theory (DFT) both in gas and aqueous phase.
21
22 Distinct arrangements possibilities were considered and their role on the stabilities
23
24 discussed based on energetic quantities and structural analysis. The understanding of
25
26 intermolecular host-guest interactions is very important, since the hydrogen bonding
27
28 must be described using an adequate treatment of electron correlation that can be
29
30 satisfactorily achieved by theoretical methods. In addition, our results can be relevant to
31
32 elucidate the elution order of 4-OH-Prop enantiomers by CE using CM- β -CD as chiral
33
34 selector. It is important to mention that, for the best of our knowledge, the present work
35
36 reports for the first time, a high level *ab initio* calculations to investigate the process
37
38 involving the formation of inclusion complex between 4-OH-Prop enantiomers and
39
40
41
42
43
44
45
46
47
48
49
50
51
52
53
54
55
56
57
58
59
60
CM- β -CD.

2 Experimental

2.1 Standard solutions and chemicals

52
53
54
55
56
57
58
59
60
Rac-4-hydroxypropranolol (4-OH-Prop, 98%) was obtained from Toronto
Research Chemicals® (North York, Canada). Stock standard solutions of 4-OH-Prop
were prepared in methanol at concentrations of 200.0 $\mu\text{g mL}^{-1}$. The standard solutions

1
2
3 were stored at -20°C in the absence of light. CM- β -CD was obtained from Fluka[®]
4
5 (Buchs, Switzerland). Triethylamine (TEA) was purchased from J. T. Baker
6
7 (Phillipsburg, USA) and phosphoric acid (H_3PO_4 , 85% in water) was obtained from
8
9 Labsynth[®] (Diadema, Brazil). Sodium hydroxide was purchased from Nuclear[®]
10
11 (Diadema, Brazil). All other chemicals were of analytical-grade in the highest purity
12
13 available. Water was distilled and purified using a Millipore[®] Milli-Q Plus system
14
15 (Bedford, USA).
16
17
18
19

20 21 2.2 Instrumentation and electrophoretic conditions

22
23 Analyses were conducted in a CE system from Agilent[®] Technologies, model
24
25 61600A (Waldbronn, Germany) consisting of an analyzer, an automatic sampler, a
26
27 diode array detector (wavelength set at 210 nm for the detection of the analytes), and an
28
29 Agilent[®] ChemStation for data acquisition. A fused silica uncoated capillary
30
31 (MicroSolv[®] Technology Corporation, Eatontown, USA) 50 μm i.d., 50 cm in total
32
33 length, and 41.5 cm in effective length was used. Before the first use, the capillary was
34
35 conditioned by rinsing with 1.0 mol L^{-1} NaOH for 10 min at 20°C , followed by
36
37 0.1 mol L^{-1} NaOH for 10 min at 20°C , and water for 10 min at 20°C . At the beginning of
38
39 each working day, the capillary was rinsed with NaOH 0.1 mol L^{-1} for 10 min followed
40
41 by water for 10 min. Between consecutive analyses, the capillary was rinsed with 0.1
42
43 mol L^{-1} NaOH for 2 min, water for 2 min, and background electrolyte for 3 min. After
44
45 daily use, the capillary was washed with 0.1 mol L^{-1} NaOH for 10 min followed by
46
47 water for 10 min. When not in use, the capillary was filled with water and its tips were
48
49 stored immersed in water.
50
51
52

53
54 The electrophoretic conditions employed in this study were previously optimized
55
56 by Box-Behnken design [5] and later the method was applied to study the Prop
57
58
59
60

1
2
3 biotransformation by endophytic fungi [6]. Briefly, the optimized conditions were as
4 follows: 4% (w/v) CM- β -CD in 25 mmol L⁻¹ TEA/H₃PO₄ buffer at pH 9 as running
5 electrolyte and 17 kV of voltage. Sample injections were performed hydrodynamically
6 at a pressure of 50 mbar for 20 s and the capillary temperature was set at 25°C. All
7 solutions used as CE running buffer and in CE rinse cycle procedure were filtered
8 through a Millex-HA 0.45 μ m disk filter from Millipore and degassed by ultrasound for
9 5 min. For more details of experimental conditions see ref. [5].
10
11
12
13
14
15
16
17
18
19

20 2.3 Elution order for 4-OH-Prop enantiomers

21 The pure enantiomers of 4-OH-Prop enantiomers were obtained using the
22 procedure previously described by Herring and Johnson [30]. Briefly, standard solutions
23 of rac-4-OH-Prop were injected into the chromatographic system, under the conditions
24 established by these authors: Chiralcel OD column and hexane: ethanol: diethylamine
25 (91: 9: 0.1%, v/v/v) as mobile phase. Under these conditions, (+)-(R)-4-OH-Prop eluted
26 later than the (-)-(S)-enantiomer. So, to establish the migration order by CE, the
27 fractions containing each enantiomer were collected at the end of the column, the
28 mobile phase was evaporated, the residues were dissolved in 25 mL of the running
29 buffer and analyzed by the electrophoretic conditions described in the present paper [5].
30
31
32
33
34
35
36
37
38
39
40
41
42
43
44

45 2.4 Computational Methodology

46 Initially, the geometries for the isolated species (+)-(R)-4-OH-Prop and (-)-(S)-
47 4-OH-Prop and CM- β -CD were fully optimized in gas phase without any geometrical or
48 symmetry constraints at BLYP/6-31G(d,p) level of theory.
49
50
51
52
53

54 Considering the inclusion process between host and guest molecules in 1:1 ratio,
55 four orientations were assumed for the CM- β -CD/4-OH-Prop complexes: *form A*, when
56
57
58
59
60

1
2
3 the 1-naphthol ring of guest molecules (4-OH-Prop) is inserted in the hydrophobic
4 cavity of the host (CM- β -CD) by the wider rim, and *form B*, when the guest is included
5 by the narrower rim of CM- β -CD, *form C*, when the aliphatic part of 4-OH-Prop is
6 inserted in the hydrophobic cavity CM- β -CD by the wider rim and *form D*, when the
7 aliphatic part of 4-OH-Prop is included by the narrower rim of CM- β -CD. **Fig. 2**
8 schematically depicts the spatial orientations of the complexes, considering the four
9 modes of inclusion. Therewith, eight distinct spatial 4-OH-Prop/CM- β -CD
10 arrangements were then generated considering the 4-OH-Prop enantiomers (R) and (S)
11 named as: (+)-(R)-4-OH-Prop/CM- β -CD (*form A*), (+)-(R)-4-OH-Prop/CM- β -CD (*form*
12 *B*), (-)-(S)-4-OH-Prop/CM- β -CD (*form A*), (-)-(S)-4-OH-Prop/CM- β -CD (*form B*), (+)-
13 (R)-4-OH-Prop/CM- β -CD (*form C*), (-)-(S)-4-OH-Prop/CM- β -CD (*form C*), (+)-(R)-4-
14 OH-Prop/CM- β -CD (*form D*) and (-)-(S)-4-OH-Prop/CM- β -CD (*form D*).

15
16
17
18
19
20
21
22
23
24
25
26
27
28
29
30
31
32
33
34
35
36
37
38
39
40
41
42
43
44
45
46
47
48
49
50
51
52
53
54
55
56
57
58
59
60

Once designed the inclusion complexes, we performed eight long length MD simulations in vacuum in order to provide detailed information on the fluctuations and conformational changes of the complexes. The simulations were carried out separately for each 4-OH-Prop/CM- β -CD complex employing the AMBER* (*Assisted Model Building with Energy Refinement*) force field. The main goal here was to obtain the global minimum geometries on the equilibrium for each complex after the MD simulations.

Once selected the equilibrium complexes geometries from MD simulations, PM3 semiempirical and Density Functional Theory (DFT) calculations were carried out in order to obtain reliable energetic properties for the inclusion process between CM- β -CD and 4-OH-Prop molecules.

The initial guess geometries for the distinct inclusion complexes arrangements were fully optimized without any geometrical or symmetry constraints at the PM3

1
2
3 semiempirical level. PM3 harmonic frequency calculations were also performed for the
4
5 equilibrium structures, characterizing them as true minima on the potential energy
6
7 surface (all frequencies are real). The PM3 frequencies were then used for the
8
9 evaluation of the internal energy (ΔE_{int}) and thermal energy (ΔG_T) corrections, with the
10
11 aid of the well known formulas of Statistical Thermodynamics [31]. We have calculated
12
13 the Gibbs free energy (ΔG) using the equations (1) and (2) below:
14
15

16
17 (1) $\Delta G = \Delta E_{\text{ele-nuc}} + \Delta G_T$

18
19 (2) $\Delta G_T = \Delta E_{\text{int}} - T\Delta S$

20
21 Afterward, the electronic plus nuclear repulsion energy contribution ($\Delta E_{\text{ele-nuc}}$)
22
23 was evaluated by DFT calculations as single point BLYP/6-31G(d,p)//PM3 calculations
24
25 using the fully optimized PM3 geometries. This sequential methodology has been
26
27 successfully used for CDs inclusion compounds in our previous works [32-34].
28

29
30 Within the quantum mechanical formalism the solvent effect was considered
31
32 using the polarized continuum model (PCM). In the condensed phase, the presence of
33
34 the solvent is replaced by its dielectric constant (for water $\epsilon = 78.35$). The solute is
35
36 placed in a cavity of suitable shape to enclose the whole molecule, which is
37
38 immediately contemplated in the continuum dielectric. The PCM single-point
39
40 calculations in solution were carried out at the BLYP/6-31 G(d,p)/PM3 level theory.
41

42
43 All theoretical calculations were carried out using Hyperchem 8.0
44
45 Computational Package and Gaussian 2009 quantum mechanical package [35].
46
47

48 49 **3. Results and discussion**

50 51 *3.1. Electrophoresis analysis*

52
53 The optimized electrophoretic conditions are summarized in Table 1 as well as
54
55 the obtained electrophoretic parameters. Chiral selectivity (a) was calculated using the
56
57
58
59
60

1
2
3 expression: $\alpha = (T_2 - T_0)/(T_1 - T_0)$; where T_2 is the migration time for the second
4
5 enantiomer, T_1 is the migration time for the first enantiomer and T_0 is the migration time
6
7 of a neutral marker, which was measured by using a system peak and/or dimethyl
8
9 sulfoxide. The software ChemStation[®] was programmed to automatically calculate the
10
11 resolution factor (R_s) and number of theoretical plates (N). The R_s (between all peaks)
12
13 and migration times were selected for the determination of the optimal conditions [5].
14
15
16
17
18

19 3.2. 4-OH-prop enantiomers inclusion in CM- β -CD

20
21 A theoretical investigation based on MD simulations, PM3 semiempirical
22
23 method and DFT calculations were performed to determine the possible 1:1
24
25 arrangements for the inclusion complexes formed by 4-OH-Prop and their respective
26
27 (+)-(R) and (-)-(S) enantiomers with CM- β -CD. Our main goal was an attempt to model
28
29 the structural and energetic parameters of the inclusion complexes, which could be used
30
31 to predict the most favorable inclusion complex conformation and consequently give us
32
33 an insight concerning the elution order 4-OH-Prop enantiomers.
34
35
36

37 As previously mentioned four distinct spatial 4-OH-Prop/CM- β -CD
38
39 arrangements were generated considering the two modes of inclusion. Each complex
40
41 was separately submitted to MD simulations in vacuum with a length of 10 ns, time step
42
43 of 1.5 fs, at temperature of 298 K using the force field AMBER*. The Results from MD
44
45 lead to a quite stable arrangement formed by host and guest molecules. In each spatial
46
47 arrangement, the electrostatic and van der Waals terms in the force field were
48
49 pronounced, accounting for almost 60% of the association energy, which ensures the
50
51 noticeable stability for the complexes association in gas phase. Thus, the global
52
53 minimum for each 4-OH-Prop/CM- β -CD arrangement obtained from de equilibrium
54
55
56
57
58
59
60

1
2
3 was used as the starting geometries submitted subsequently to semiempirical and DFT
4
5 calculations.
6

7
8 The structures of the two 4-OH-Prop/CM- β -CD complexes optimized at the
9
10 PM3 semiempirical level of theory considering the *form A* inclusion are depicted in **Fig.**
11
12 **3**. Likewise, the structures of two host-guest 4-OH-Prop/CM- β -CD complexes,
13
14 considering the *form B* inclusion, optimized at the PM3 semiempirical level of theory
15
16 are depicted in **Fig. 4**.
17

18
19 **Table 2** contains the Binding Energy (ΔE) and Gibbs Free Energy (ΔG)
20
21 evaluated at the BLYP/6-31G(d,p)//PM3 level for the inclusion process of 4-OH-Prop in
22
23 CM- β -CD, calculated both in gas and aqueous phases. Analyzing **Table 2**, more
24
25 specifically on gas phase results, one can observe from binding energy (ΔE) that the
26
27 most favorable inclusion complex, among the four possible arrangements considering
28
29 the enantiomeric species (R) and (S), was found to be the (+)-(R)-4-OH-Prop/CM- β -
30
31 CD, on *form A* spatial orientation (inclusion made from wider CD rim). The reason for
32
33 such considerable stabilization observed for this complex can be explained by a
34
35 meticulous structural analysis at the molecular level, which revealed that three strong
36
37 hydrogen bonds are established between the 4-OH-Prop hydroxyl group (located on
38
39 chiral carbon) and the secondary hydroxyl group of the CM- β -CD (see **Fig. 3a**). These
40
41 hydrogen bonds may be considered the main forces responsible for the stabilization of
42
43 the complex which leads the (+)-(R)-4-OH-Prop/CM- β -CD complex to be the most
44
45 energetically favored compared to the others three complexes. Still observing the
46
47 optimized complexes geometries shown on **Fig. 3b, 4a** and **4b** one can verify that no
48
49 intermolecular hydrogen bonds were established between host and guest molecules.
50
51 This may explains why these complexes presented lower binding energies when
52
53 compared with the (+)-(R)-4-OH-Prop/CM- β -CD specie.
54
55
56
57
58
59
60

1
2
3 The solvent effect was also considered in the PCM method using water as the
4 solution phase. The results support the previous conclusion obtained in gas phase
5 concerning not only the energetic stability order of the inclusion complexes
6 arrangements, but also the higher stability of the (+)-(R)-4-OH-Prop/CM- β -CD specie.
7 In this case, the presence of the solvent medium increases the binding energy (ΔE) by
8 5.7 kcal/mol on the stabilization of (+)-(R)-4-OH-Prop/CM- β -CD complex from gas
9 phase (-24.8 kcal/mol) to aqueous phase (-30.5 kcal/mol).
10
11
12
13
14
15
16
17
18

19 The Gibbs free energy (ΔG) was also evaluate by combining the BLYP/6-
20 31G(d,p)//PM3 $\Delta E_{\text{ele-nuc}}$ values with the PM3 ΔE_{int} and ΔG_{T} quantities using Statistical
21 Thermodynamics (eqs. 1 and 2). The calculated ΔG values both in gas phase and
22 aqueous solution are also reported in **Table 2**. The ΔG negative values encountered for
23 all four complexes, on both phases, indicated the binding spontaneity of the guest
24 molecule to the host. Besides, the ΔG results also pointed out that the (+)-(R)-4-OH-
25 Prop/CM- β -CD should be preferred based on energetic grounds on both phases, at the
26 normal pressure and room temperature. Taking to account the solvent effect on ΔG
27 values, the results clearly shown the same behavior obtained in the gas phase regarding
28 not only to the spontaneity order of the inclusion complexes arrangements, but also to
29 the higher spontaneity of the (+)-(R)-4-OH-Prop/CM- β -CD specie. In this case, the
30 presence of the solvent medium increases by 3.7 kcal/mol the ΔG of (+)-(R)-4-OH-
31 Prop/CM- β -CD complex from gas phase (-5.7 kcal/mol) to solvent phase (-9.4
32 kcal/mol).
33
34
35
36
37
38
39
40
41
42
43
44
45
46
47
48
49
50

51 From **Table 2** results, it is also interesting to point out though that these
52 inclusion modes by the aliphatic group inclusion were not participating at the
53 enantiomers separation, once their stability differences are insignificant, being less or
54 equal
55
56
57
58
59
60

1
2
3 1 kcal mol⁻¹ at aqueous phase. Also, these structures should not be present as inclusion
4 products because of the formation free energies are all positive. Besides the
5 thermodynamic analysis, we can also observe the optimized structures for these
6 inclusion complexes as depicted in **Figure 5** and check out the intermolecular
7 interactions formed by the guest inclusion. Looking into the complexes arrangements
8 there are not hydrogen bond established between host and guest in any of those
9 structures. So, according to the **Table 2** data, these complexes show no attractive
10 intermolecular interactions that could be source for an energetic stabilization or to take
11 them into account to the equilibrium involved in this work. These results corroborate the
12 fact that aromatic part is more favored and so on, responsible for the enantiomer
13 migration order differences.
14
15
16
17
18
19
20
21
22
23
24
25
26
27
28

29 3.3. *4-OH-prop enantiomers inclusion in β -CD*

30
31 All cyclodextrins are recognized as chiral selectors, the native ones, however,
32 are less selective, so modified ones are being employed with more success. The use of
33 CM- β -CD as chiral selector in detriment to native one has experimental reasons as for
34 example, stabilization in different pH range and also increasing on the electrophoretic
35 mobility. On the other hand, the stabilized interactions provided by the modified
36 cyclodextrin are not involving the carbomethyl group being described though by
37 secondary hydroxyl groups. Thus, the results for native β -CD inclusion complexes were
38 pretty similar to those reported for 4-OH-Prop /CM- β -CD complexes. The choice by
39 CM- β -CD is more attractive due to its solubility in water (or background solution -
40 BGS) to be higher than the β -CD. **Table 3** summarized the thermodynamic parameters
41 obtained in this analysis.
42
43
44
45
46
47
48
49
50
51
52
53
54
55
56
57
58
59
60

1
2
3 The complex (+)-(R)-4-OH-Prop/ β -CD (*form A*) is the only one which shows
4
5 spontaneous thermodynamics among four complexes calculated. Besides this result, β -
6
7 CD would be indeed used as chiral selector, just using the relative stability of the
8
9 preferred enantiomer and the presence of two hydrogen bonds, as visualized in **Figure**
10
11 **6**. These interactions are quite in the same arrangement observed for the CM- β -CD
12
13 complex.
14
15

16 17 18 3.4. *Molecular modeling for elution order elucidation*

19
20 It is important to highlight that the binding energies and Gibbs free energies
21
22 results for the species in solution can be regarded as a fair estimative of the enthalpy
23
24 values for the inclusion process in solution. These theoretical data are quite useful for
25
26 the experimentalist, since a direct relationship of the thermodynamic quantity with a
27
28 specific spatial molecular arrangement for the inclusion complex is made, and so, an
29
30 understanding of the intermolecular interactions in solution at a molecular level is
31
32 possible.
33
34

35
36 The obtained results showed that (+)-(R)-4-OH-Prop/CM- β -CD complex in both
37
38 gas and solvent phase was more energetically favorable (lower ΔE and ΔG values). This
39
40 significant difference in energies detected for the inclusion process of 4-OH-Prop with
41
42 CM- β -CD can be a fair measure of chiral discrimination, which results in the separation
43
44 of the enantiomers and the different separation factors as observed in our previous
45
46 experimental studies [5,6]. In addition, the presence of water as solvent did not interfere
47
48 in enantiomer migration order, which does not discard this kind of study for other
49
50 molecules and conditions. Finally, one can notice that the inclusion by the wider CDs
51
52 cavity (*form A*) is the most stable arrangement regardless the enantiomer observed.
53
54
55
56
57
58
59
60

1
2
3 The elution order for 4-OH-Prop enantiomers was established based on the
4 methods previously reported in literature [5, 6, 30]. The migration order for the
5 electrophoretic conditions obtained in our previous papers is in complete accordance
6 with the theoretical results reported, since the as EMO for 4-OH-Prop enantiomers was:
7
8 (1) (-)-(S)-4-OH-Prop and (2) (+)-(R)-4-OH-Prop (Fig. 7). Therefore, the molecular
9 modeling techniques provides us with a good perspective of enantioseparation and
10 serves as a useful method for studying chiral recognition mechanisms and predicting
11 chiral separation.
12
13
14
15
16
17
18
19

20 21 22 23 4. CONCLUSIONS

24
25 In the present study MD simulations, PM3 semiempirical and DFT calculations
26 were performed for the inclusion process of 4-OH-Prop in CM- β -CD. As result we
27 described energetic parameters for the inclusion complexes at a molecular level which
28 were in good agreement with the experimental findings concerning the elution order of
29 guest 4-OH-Prop enantiomers. In addition, a systematic structural analysis indicated that
30 hydrogen bonds formed between host and guests played a major role on the complex
31 stabilization. Moreover, the difference in energies of drug/CM- β -CD inclusion
32 complexes, concerning the 4-OH-Prop enantiomers and the two distinct modes of
33 inclusion, is probably a measure of chiral discrimination, which results in the separation
34 of the enantiomers and the distinct separation factors as observed in the previous
35 experimental studies.
36
37
38
39
40
41
42
43
44
45
46
47
48
49
50
51
52
53
54
55
56
57
58
59
60

Acknowledgements

The authors would like to thank the Brazilian agencies CNPq (Conselho Nacional de Desenvolvimento Científico e Tecnológico), CAPES (Coordenação de Aperfeiçoamento de Pessoal de Nível Superior) and FAPEMIG (Fundação de Amparo à Pesquisa do Estado de Minas Gerais) for financial support. This study is also part of the project involving the Rede Mineira de Química (RQ-MG) supported by FAPEMIG (Project: REDE-113/10).

References

- [1] R. Bhushan, S. Tanwar, *Biomed. Chromatogr.* 2008, **22**, 1028 – 1034.
- [2] R. Bhushan, S. Tanwar, *J. Chromatogr. A* 2010, **1217**, 1395 – 1398.
- [3] A.A. Younes, D. Mangelings, Y.V. Heyden, *J. Pharm. Biomed. Anal.*, 2011, **55**, 414 – 423.
- [4] I. Ali, V.D. Gaitonde, H.Y. Aboul-Enein, A. Hussain, *Talanta*, 2009, **78**, 458 – 463.
- [5] K.B. Borges, M.T. Pupo, L.A.P. de Freitas, P.S. Bonato, *Electrophoresis*, 2009, **30** 2874 – 2881.
- [6] K.B. Borges, M.T. Pupo, P.S. Bonato, *Electrophoresis*, 2009, **30**, 3910 – 3917.
- [7] P. Shahgaldian, U. Pieleles, *Sensors*, 2006, **6**, 593 – 615.
- [8] T. de Boer, R.A. de Zeeuw, G.J. De Jong, K. Ensing, *Electrophoresis*, 2000, **21**, 3220 – 3239.
- [9] A.-C. Servais, A. Rousseau, M. Fillet, K. Lomsadze, A. Salgado, J. Crommen, B. Chankvetadze, *Electrophoresis*, 2010, **31**, 1467 – 1474.
- [10] A.-C. Servais, A. Rousseau, M. Fillet, K. Lomsadze, A. Salgado, J. Crommen, B. Chankvetadze, *J. Sep. Sci.*, 2010, **33**, 1617 – 1624.
- [11] A.A. Elbashir, F.E.O Suliman, *J. Chromatogr. A*, 2011, **1218**, 5344 – 5351.
- [12] E.E.M. Eid, A.B. Abdul, F.E.O. Suliman, M.A. Sukari, A. Rasedee, S.S. Fatah, *Carbohydr. Polym.*, 2011, **83**, 1707 – 1714.
- [13] C. Jullian, M. Alfaro, G. Zapata-Torres, C. Olea-Azar, *J. Solut. Chem.*, 2010, **39**, 1168 – 1177.
- [14] S. Chaudhuri, S. Chakraborty, P.K. Sengupta, *J. Mol. Struct.*, 2010, **975**, 160 – 165.
- [15] Z. Bikádi, G. Fodor, I. Hazai, P. Hári, J. Szemán, L. Szente, F. Fülöp, A. Péter, E. Hazai, *Chromatographia*, 2010, **71**, 21 – 28.

- 1
2
3 [16] E. Bednarek, W. Bocian, K. Michalska, J. Chromatogr. A, 2008, **1193**, 164 – 171.
4
5 [17] W. Li, C. Liu, G. Tan, X. Zhang, Z. Zhu, Y. Chai, Int. J. Mol. Sci., 2012, **13**, 710 –
6
7 725.
8
9 [18] B. Natalini, N. Giacchè, R. Sardella, F. Ianni, A. Macchiarulo, R. Pellicciari, J.
10 Chromatogr. A, 2010, **1217**, 7523 – 7527.
11
12 [19] W. Li, G. Tana, L. Zhaoc, X. Chena, X. Zhanga, Z. Zhua, Y. Chaia, Anal. Chim.
13 Acta, 2012, **718**, 138 – 144.
14
15 [20] B. Chankvetadze, Electrophoresis, 2002, **23**, 4022 – 4035.
16
17 [21] B. Chankvetadze, G. Schulte, G. Blaschke, Enantiomer, 1997, **2**, 157 – 178.
18
19 [22] P.A. Bond, Nature, 1967, **213**, 721 – 721.
20
21 [23] J.D. Fitzgerald, S.R. O'Donnell, Br. J. Pharmacol., 1971, **43**, 222 – 235.
22
23 [24] C.R. Clevaveland, D.G. Shand, Clin. Pharmacol. Ther., 1972, **13**, 181 – 185.
24
25 [25] J.W. Paterson, M.E. Connolly, C.T. Dollery, A. Hayes, R.G. Cooper, Eur. J. Clin.
26 Pharmacol., 1970, **2**, 127 – 133.
27
28 [26] D.G. Shand, E.M. Nuckolls, J.A. Oates, Clin. Pharmacol. Ther., 1970, **11**, 112 –
29 120.
30
31 [27] T. Walle, U.K. Walle, T.D. Cowart, E.C. Conradi, T.E. Gaffney, J. Pharmacol.
32 Exp. Ther., 1987, **241**, 928 – 933.
33
34 [28] B. Silber, N.H.G. Holford, S. Riegelman, J. Pharm. Sci., 1982, **71**, 699 – 704.
35
36 [29] A. Hayes, R.G. Cooper, J. Pharmacol. Exp. Ther., 1971, **176**, 302 – 311.
37
38 [30] V.L. Herring, J.A. Johnson, J. Chromatogr., 1993, **612**, 215 – 221.
39
40 [31] D. A. McQuarrie, *Statistical Thermodynamics*, University Science Books, Mill
41 Valley, 1973.
42
43 [32] C.S. Nascimento Jr., C.P.A. Anconi, H.F. dos Santos, W.B. de Almeida, J. Phys.
44 Chem. A, 2005, 109, 3209 – 3219.
45
46
47
48
49
50
51
52
53
54
55
56
57
58
59
60

1
2
3 [33] C.S. Nascimento Jr., H.F. dos Santos, W.B. de Almeida, Chem. Phys. Lett., 2004,
4
5 397, 422 – 428.

6
7 [34] F.B. de Sousa, C.S. Nascimento Jr., W.B. de Almeida, R.D. Sinisterra, J. Am.
8
9 Chem. Soc., 2008, **130**, 8426 – 8436.

10
11 [35] M.J. Frisch, G.W. Trucks, H.B. Schlegel, G.E. Scuseria, M.A. Robb, J.R.
12
13 Cheeseman, G. Scalmani, V. Barone, B. Mennucci, G.A. Petersson, H. Nakatsuji, M.
14
15 Caricato, X. Li, H.P. Hratchian, A.F. Izmaylov, J. Bloino, G. Zheng, J.L. Sonnenberg,
16
17 M. Hada, M. Ehara, K. Toyota, R. Fukuda, J. Hasegawa, M. Ishida, T. Nakajima, Y.
18
19 Honda, O. Kitao, H. Nakai, T. Vreven, J.A. Montgomery Jr., J.E. Peralta, F. Ogliaro, M.
20
21 Bearpark, J.J. Heyd, E. Brothers, K.N. Kudin, V.N. Staroverov, R. Kobayashi, J.
22
23 Normand, K. Raghavachari, A. Rendell, J.C. Burant, S.S. Iyengar, J. Tomasi, M. Cossi,
24
25 N. Rega, J.M. Millam, M. Klene, J.E. Knox, J.B. Cross, V. Bakken, C. Adamo, J.
26
27 Jaramillo, R. Gomperts, R.E. Stratmann, O. Yazyev, A.J. Austin, R. Cammi, C. Pomelli,
28
29 J.W. Ochterski, R.L. Martin, K. Morokuma, V.G. Zakrzewski, G.A. Voth, P. Salvador,
30
31 J.J. Dannenberg, S. Dapprich, A.D. Daniels, Ö. Farkas, J.B. Foresman, J.V. Ortiz, J.
32
33 Cioslowski, D.J. Fox, Gaussian 2009, revision A.02, Gaussian, Inc., Wallingford CT,
34
35 2009.
36
37
38
39
40
41
42
43
44
45
46
47
48
49
50
51
52
53
54
55
56
57
58
59
60

Figure Captions

Fig. 1. Molecular structure of 4-hydroxypropranolol (4-OH-Prop) enantiomers (the chiral centers are indicated by an asterisk) and CM- β -CD.

Fig. 2. Modes of inclusion (a) *form A*: naphthyl ring of 4-OH-Prop is inserted in the hydrophobic cavity CM- β -CD by the wider rim; (b) *form B*: naphthyl ring of 4-OH-Prop is included by the narrower rim of CM- β -CD; (c) *form C*: aliphatic part of 4-OH-Prop is inserted in the hydrophobic cavity CM- β -CD by the wider rim; (d) *form D*: aliphatic part of 4-OH-Prop is included by the narrower rim of CM- β -CD. The R- in figure represents carboxymethyl group.

Fig. 3. PM3 fully optimized structures for 4-OH-Prop/CM- β -CD inclusion complexes arrangements. The geometries are depicted in two views (front and side): (a) (+)-(R)-4-OH-Prop/CM- β -CD (*form A*) and (b) (-)-(S)-4-OH-Prop/CM- β -CD (*form A*). The dashed lines represent the intermolecular hydrogen bonds (three bonds) established between host and guest. The zoomed image is also depicted to highlight the H-bonds.

Fig. 4. PM3 fully optimized structures for 4-OH-Prop/CM- β -CD inclusion complexes arrangements. The geometries are depicted in two views (front and side). (a) (+)-(R)-4-OH-Prop/CM- β -CD (*form B*) and (b) (-)-(S)-4-OH-Prop/CM- β -CD (*form B*).

Fig. 5. PM3 fully optimized structures for 4-OH-Prop/CM- β -CD aliphatic modes of inclusion complexes. The geometries are depicted in two views (front and side): a) (+)-(R)-4-OH-Prop/CM- β -CD (*form C*) and (b) (-)-(S)-4-OH-Prop/CM- β -CD (*form D*).

1
2
3
4
5 **Fig. 6.** (+)-(R)-4-OH-Prop/ β -CD (*form A*) optimized PM3. The dashed lines represent
6
7
8 the two hydrogen bonds formed between host and guest.
9

10
11 **Fig. 7.** Electropherograms of TEA buffer (a) and 4-OH-Prop enantiomers (b). (1) (-)-
12
13 (S)-4-OH-Prop; (2) (+)-(R)-4-OH-Prop. Conditions: TEA buffer concentration 25 mM,
14
15
16 buffer pH 9, 4% of CM- β -CD and voltage of 17 kV. Other conditions see item 2.2.
17
18
19
20
21
22
23
24
25
26
27
28
29
30
31
32
33
34
35
36
37
38
39
40
41
42
43
44
45
46
47
48
49
50
51
52
53
54
55
56
57
58
59
60

Tables

Table 1. Electrophoretic parameters for the resolution of 4-OH-Prop enantiomers using 4% CM- β -CD in 25 mM TEA/H₃PO₄ buffer at pH 9 as running electrolyte and 17 kV of voltage.^{a)}

Parameters	(-)-(S)-4-OH-Prop	(+)-(R)-4-OH-Prop
Migration time (min)	13.25	13.61
μA (cm ² /V s) ^{b)}	1.52×10^{-4}	1.47×10^{-4}
μE (cm ² /V s) ^{c)}	-1.33×10^{-4}	-1.37×10^{-4}
N	67 537	63 456
R_s		2.02
α		1.08

a) Electrosmotic mobility, μEOF (cm²/V s) = 2.86×10^{-4} , T_{EOF} = 7.10 min, l = 41.5 cm, L = 50.0 cm and V = 17 000 V. The other conditions: hydrodynamic injections at a pressure of 50 mbar for 20 s and the capillary temperature was set at 25°C.

b) Apparent mobilities.

c) Electrophoretic mobility.

Table 2. Binding Energy (ΔE) and Gibbs Free Energy (ΔG) calculated by BLYP/6-31G(d,p)//PM3 level of theory for inclusion complexes formed by 4-OH-Prop enantiomers with CM- β -CD.

Inclusion Complexes (forms)	BLYP/6-31G(d,p)//PM3 ^{a)}							
	Gas Phase (kcal/mol)				Aqueous Phase (kcal/mol)			
	ΔE	$ \Delta\Delta E $ ^{b)}	ΔG	$ \Delta\Delta G $ ^{c)}	ΔE	$ \Delta\Delta E $ ^{b)}	ΔG	$ \Delta\Delta G $ ^{c)}
(+)-(R)-4-OH-Prop/CM- β -CD (<i>form A</i>)	-24.8		-5.7		-30.5		-9.4	
(-)-(S)-4-OH-Prop/CM- β -CD (<i>form A</i>)	-13.1	11.7	-2.5	3.2	-16.9	13.7	-4.2	5.2
(+)-(R)-4-OH-Prop/CM- β -CD (<i>form B</i>)	-13.9		-3.8		-15.1		-5.0	
(-)-(S)-4-OH-Prop/CM- β -CD (<i>form B</i>)	-12.0	1.9	-2.0	1.8	-13.7	1.8	-2.9	2.1
(+)-(R)-4-OH-Prop/CM- β -CD (<i>form C</i>)	-3.3		5.7		-6.4		4.6	
(-)-(S)-4-OH-Prop/CM- β -CD (<i>form C</i>)	-2.5	0.8	6.5	1.2	-4.6		5.6	1.0
(+)-(R)-4-OH-Prop/CM- β -CD (<i>form D</i>)	-2.9		6.3		-5.3		5.5	
(-)-(S)-4-OH-Prop/CM- β -CD (<i>form D</i>)	-2.3	0.6	7.2	0.9	-3.8	1.5	6.2	0.7

a) Values in kcal/mol estimated on 298.15 K and 1 atm;

b) $|\Delta\Delta E|$ as referred to relative interaction energies between 4-OH-Prop enantiomers (R) and (S);

c) $|\Delta\Delta G|$ as referred to relative interaction Gibbs free energy between 4-OH-Prop enantiomers (R) and (S).

Table 3. Binding Energy (ΔE) and Gibbs Free Energy (ΔG) calculated by BLYP/6-31G(d,p)//PM3 level of theory for inclusion complexes formed by 4-OH-Prop enantiomers with native β -CD.

Inclusion Complexes (forms)	BLYP/6-31G(d,p)//PM3 ^{a)}							
	Gas Phase (kcal/mol)				Aqueous Phase (kcal/mol)			
	ΔE	$ \Delta\Delta E $ ^{b)}	ΔG	$ \Delta\Delta G $ ^{c)}	ΔE	$ \Delta\Delta E $ ^{b)}	ΔG	$ \Delta\Delta G $ ^{c)}
(+)-(R)-4-OH-Prop/ β -CD (<i>form A</i>)	-18.5		-1.3		-25.4		-3.8	
(-)-(S)-4-OH-Prop/ β -CD (<i>form A</i>)	-8.6	9.9	2.5	3.8	-12.6	12.8	1.7	5.5
(+)-(R)-4-OH-Prop/ β -CD (<i>form B</i>)	-8.4		2.3		-12.1		1.4	
(-)-(S)-4-OH-Prop/ β -CD (<i>form B</i>)	-7.4	1.0	3.6	1.3	-10.7	1.4	2.9	1.5

a) Values in kcal/mol estimated on 298.15 K and 1 atm;

b) $|\Delta\Delta E|$ as referred to relative interaction energies between 4-OH-Prop enantiomers (R) and (S);

c) $|\Delta\Delta G|$ as referred to relative interaction Gibbs free energy between 4-OH-Prop enantiomers (R) and (S).

Figure 1

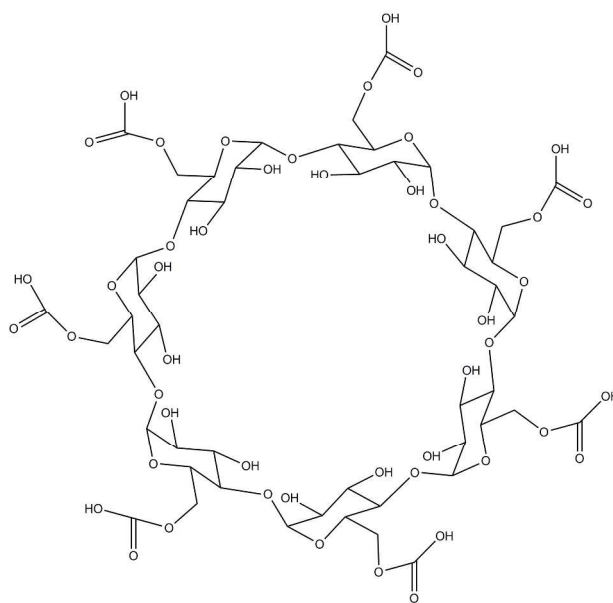
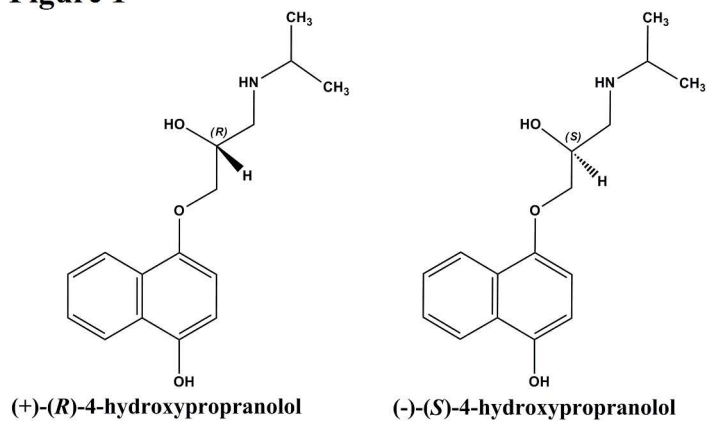


Fig. 1. Molecular structure of 4-hydroxypropranolol (4-OH-Prop) enantiomers (the chiral centers are indicated by an asterisk) and CM- β -CD.
567x924mm (96 x 96 DPI)

Figure 2

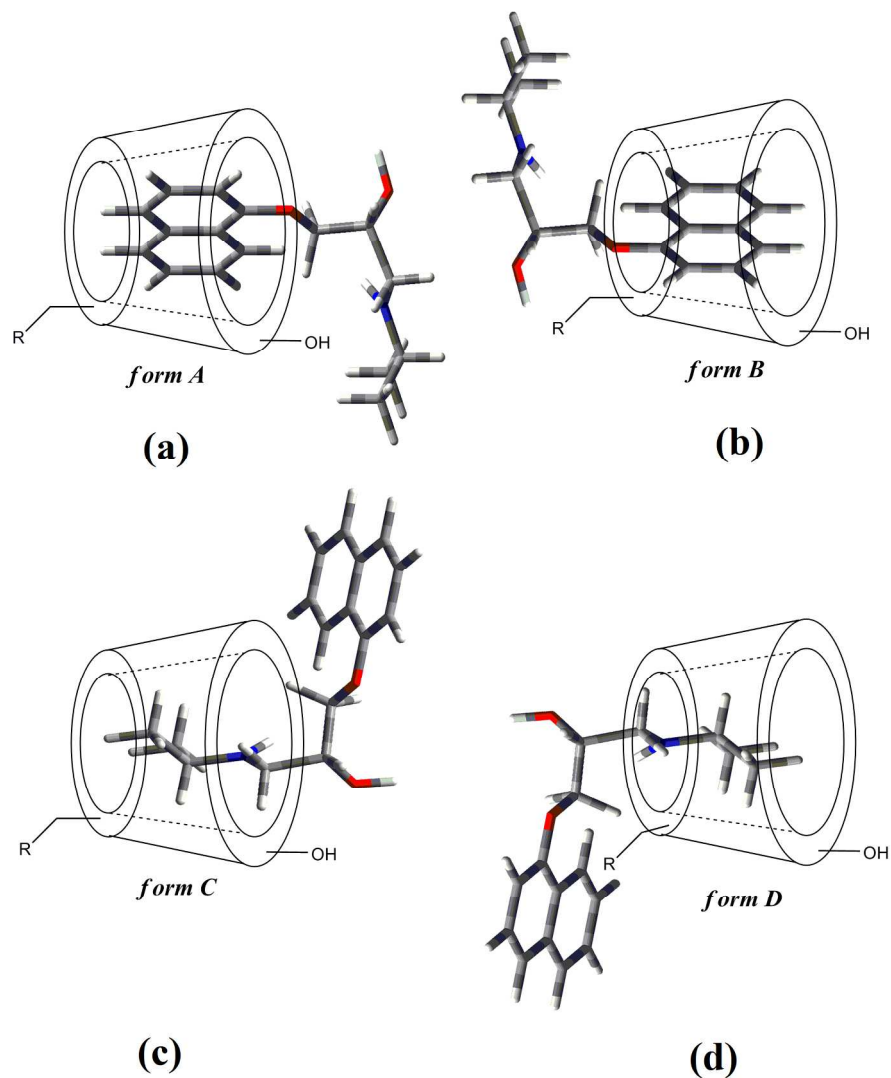


Fig. 2. Modes of inclusion (a) form A: naphtyl ring of 4-OH-Prop is inserted in the hydrophobic cavity CM-β-CD by the wider rim; (b) form B: naphtyl ring of 4-OH-Prop is included by the narrower rim of CM-β-CD; (c) form C: aliphatic part of 4-OH-Prop is inserted in the hydrophobic cavity CM-β-CD by the wider rim; (d) form D: aliphatic part of 4-OH-Prop is included by the narrower rim of CM-β-CD. The R- in figure represents carboxymethyl group.
194x242mm (300 x 300 DPI)

Figure 3

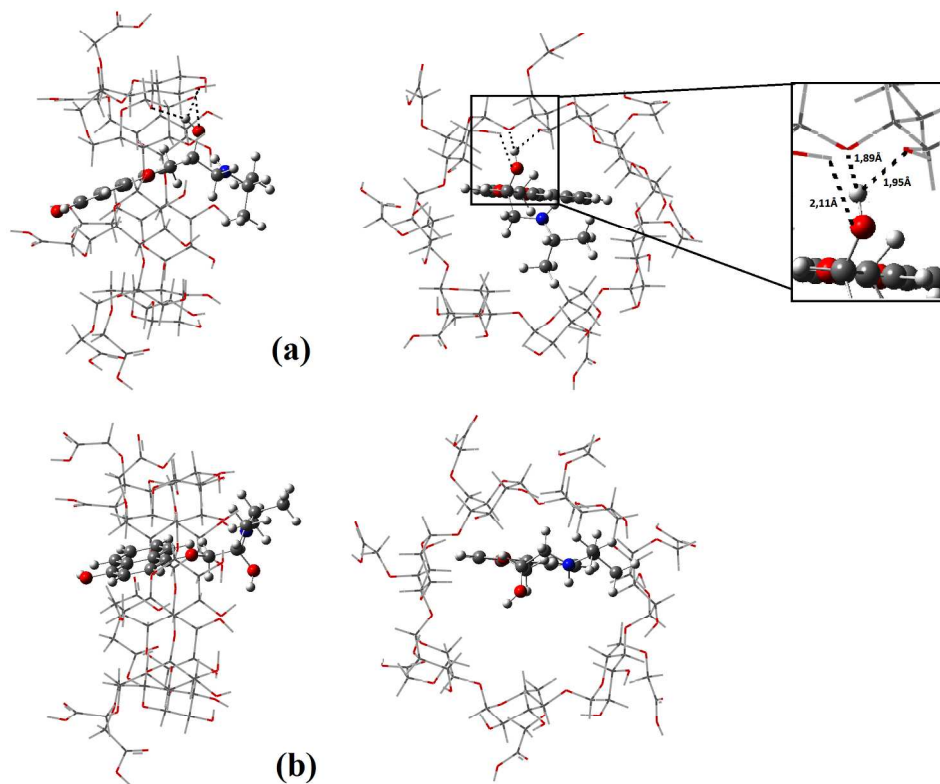


Fig. 3. PM3 fully optimized structures for 4-OH-Prop/CM-β-CD inclusion complexes arrangements. The geometries are depicted in two views (front and side): (a) (+)-(R)-4-OH-Prop/CM-β-CD (form A) and (b) (-)-(S)-4-OH-Prop/CM-β-CD (form A). The dashed lines represent the intermolecular hydrogen bonds (three bonds) established between host and guest. The zoomed image is also depicted to highlight the H-bonds. 620x545mm (96 x 96 DPI)

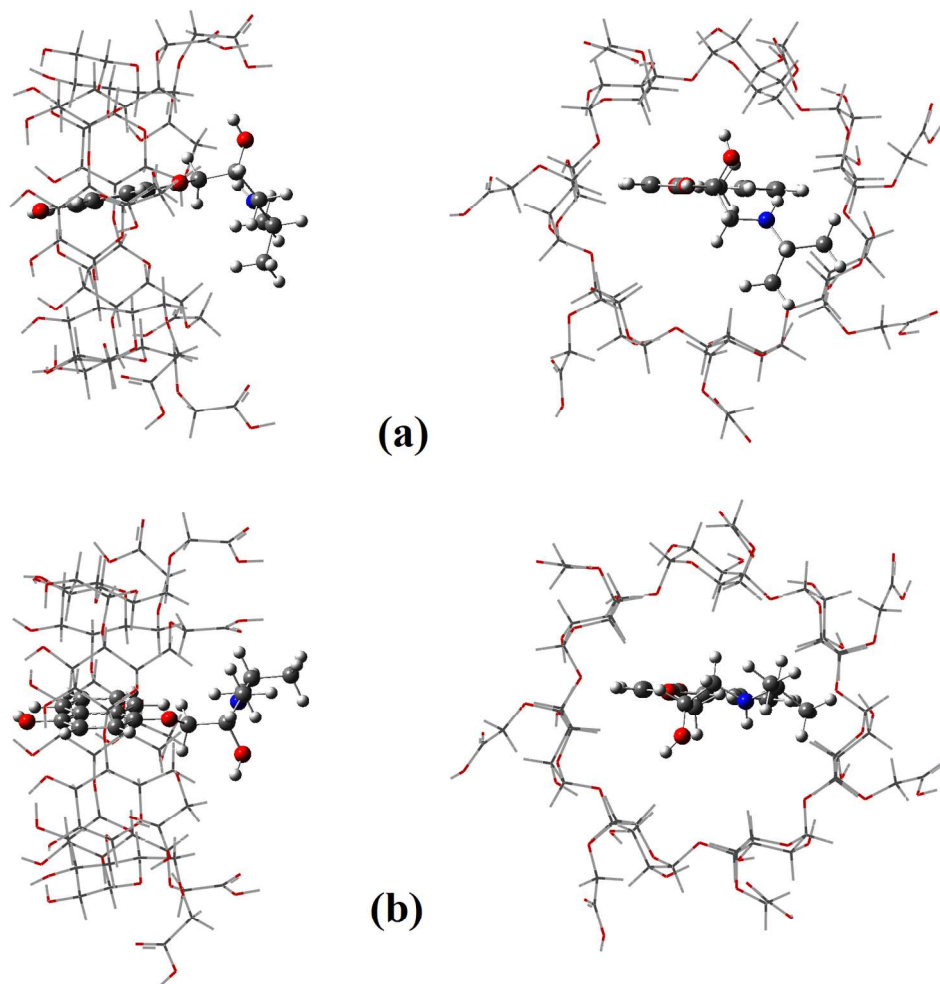
Figure 4

Fig. 4. PM3 fully optimized structures for 4-OH-Prop/CM-β-CD inclusion complexes arrangements. The geometries are depicted in two views (front and side). (a) (+)-(R)-4-OH-Prop/CM-β-CD (form B) and (b) (-)-(S)-4-OH-Prop/CM-β-CD (form B).
480x537mm (96 x 96 DPI)

Figure 5

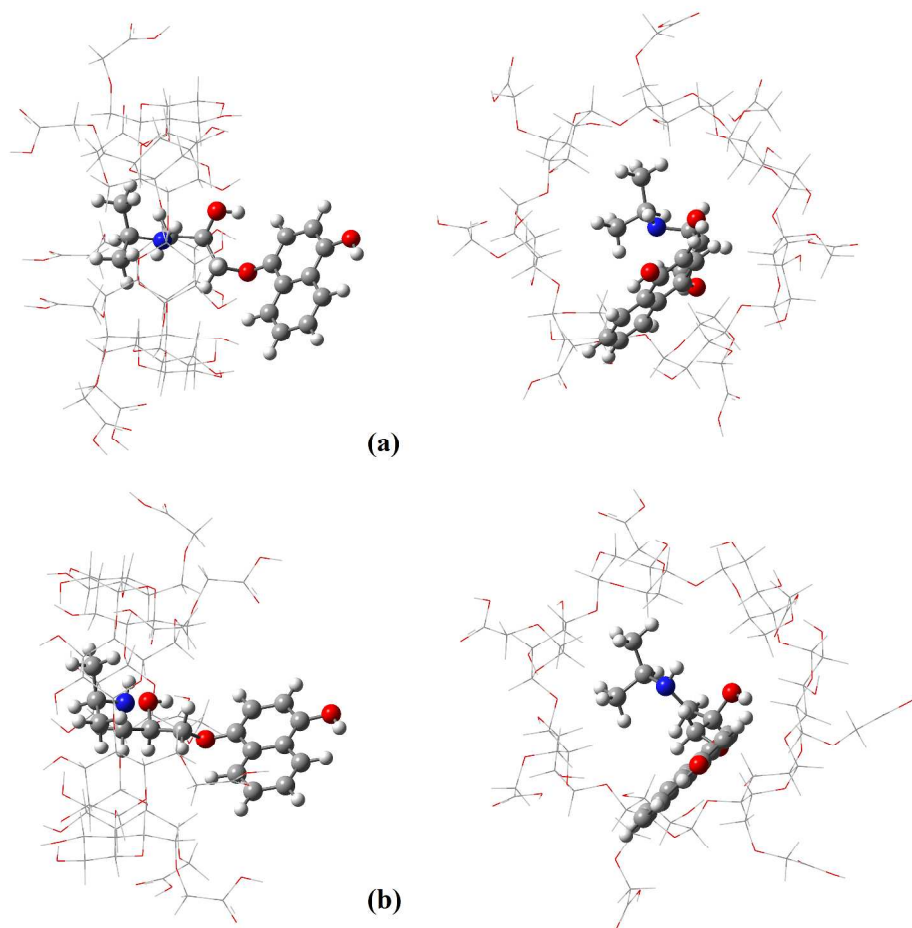


Fig. 5. PM3 fully optimized structures for 4-OH-Prop/CM- β -CD aliphatic modes of inclusion complexes. The geometries are depicted in two views (front and side): a) (+)-(R)-4-OH-Prop/CM- β -CD (form C) and (b) (-)-(S)-4-OH-Prop/CM- β -CD (form D).
1126x1143mm (96 x 96 DPI)

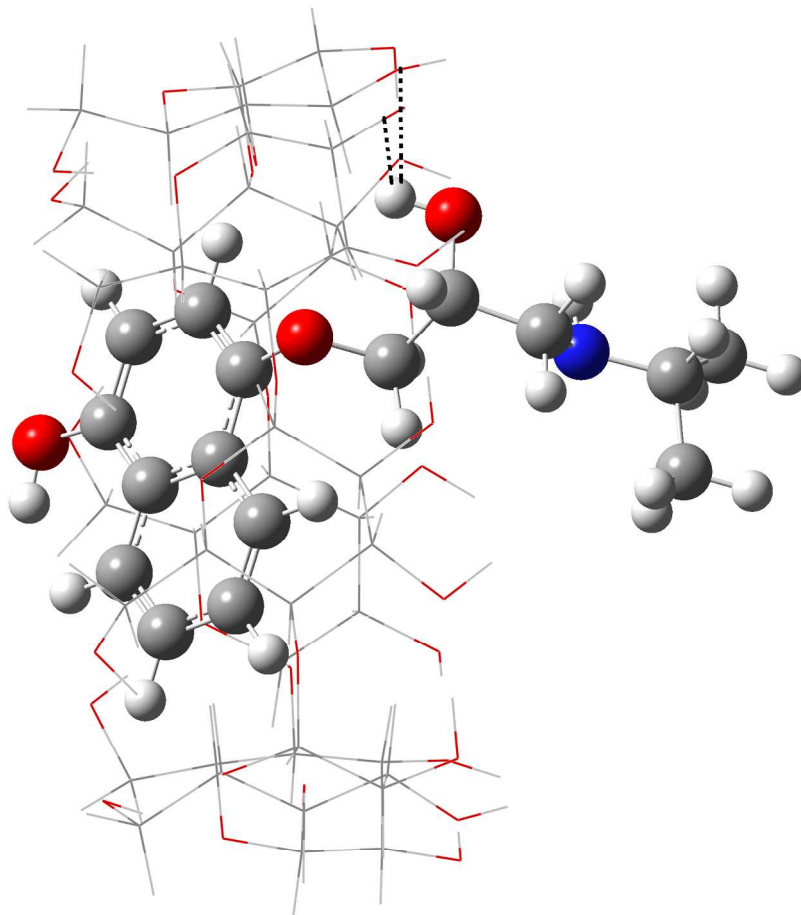
Figure 6

Fig. 6. (+)-(R)-4-OH-Prop/β-CD (form A) optimized PM3. The dashed lines represent the two hydrogen bonds formed between host and guest.
549x565mm (96 x 96 DPI)

Figure 7

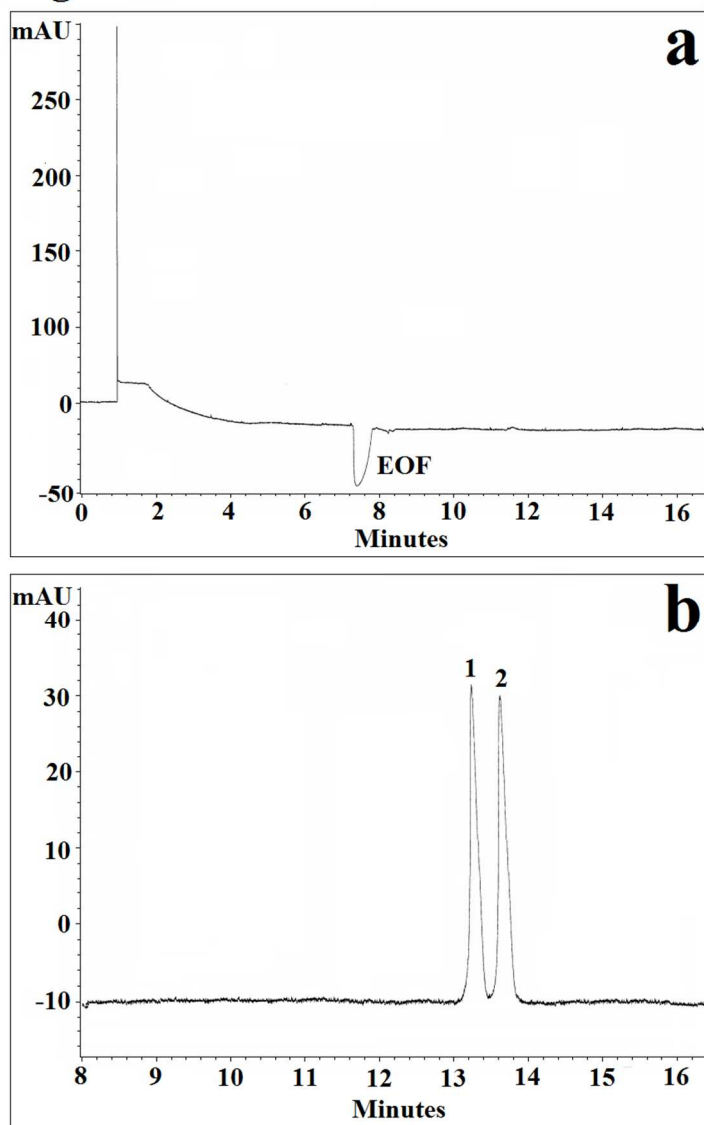


Fig. 7. Electropherograms of TEA buffer (a) and 4-OH-Prop enantiomers (b). (1) (-)-(S)-4-OH-Prop; (2) (+)-(R)-4-OH-Prop. Conditions: TEA buffer concentration 25 mM, buffer pH 9, 4% of CM- β -CD and voltage of 17 kV. Other conditions see item 2.2.
242x382mm (96 x 96 DPI)